Original scientific paper

SIMULATION OF A SINGLE THIRD-BODY PARTICLE IN FRICTIONAL CONTACT

Qiang Li

Berlin University of Technology, Berlin, Germany

Abstract. *Contact of a single third-body particle between two plates is simulated using the Boundary Element Method. The particle is considered as deformable, and the Coulomb's law of friction is assumed at the contact interface. The normal pressure distribution and tangential stress distribution in contact as well as the macroscopic force and force moment are calculated. Several movement modes are shown to be possible: rolling, rotation, or sticking during the loading. It is found that, differing from rigid particles, the state of particle may change during the loading. The particle may stick to the plates initially, but rotation may occur when the load becomes larger. Examples with the same and different coefficients of friction are presented to show kinematics of particle. The method can be further applied to simulation of multiple third-body particles.*

Key Words: *Third-body, Particle, Friction, Numerical Simulation, Boundary Element Method*

1. INTRODUCTION

It is the mechanics of interactions between the surfaces of contacting bodies which determines the tribological properties in contact. The processes occurring in the "interface" are multiple and complex: material transfer, wear, friction, particle formation, oxidation and corrosion, heat transfer, fluid flow and many others [1]. The so-called "third-body" - immediate vicinity of an interface, including the surface layers of the bodies and the particles in the interface volume - plays a significant role in terms of tribological properties. The interface particles and interfacial materials develop during the frictional process and are usually unmeasurable. Therefore, a very common way to study third-body is experimentally measuring the coefficient of friction and wear rate for different materials, loading and system parameters and surrounding environment [2, 3]. Experimental studies have shown that the wear particle flow is essential for the formation, localization, and reconstitution of load-bearing structures or films as well as the resulting friction and wear rate [4]. There have

been only few analytical and numerical studies of the third body processes due to complicated interactions among the moving surfaces and the intermedia. The Molecular Dynamic (MD) simulation is usually used for simulating interaction of atom layers and particles in a micro scale [5, 6]. Recently the Monte Carlo method has been used to predict the three-body abrasive wear rate [7], Cellular Automata for evaluation of wear particle flow and load and temperature distribution [8]. Due to the complicated third-body processes sometimes only one aspect for obtaining a basic understanding of its role is considered, for example only adhesion or friction without wear and lubrication [9, 10]. In this study, we focus on frictional contact of deformable particles between the rigid plates which is numerically simulated by using the Boundary Element Method (BEM).

BEM is an effective numerical simulation method for solving contact problems, especially assisted by the Fast Fourier Transform [11]. It has been applied to various tribological problems in the last twenty years, including indentation test, partial sliding and adhesive contact, etc. [12-14]. Recently it has been further developed to layered system [15], power-law graded materials [16] and arbitrary two-dimensional shapes [17]. However, it has been rarely used for contact of third-body particles. In this work we consider a single soft particle compressed by two parallel plates. Under the loading the particle could roll, rotate or keep unmoved (sticking). The normal and tangential stress distribution as well as its moment will be calculated for determination of particle state.

2. METHODS

We consider a single particle trapped between two plates, as shown in Fig. 1. The following assumptions are made in the study: (1) deformation of a particle is elastic; (2) particle is massless (meaning that we consider the quasistatic processes). It is further assumed that due to chemical reaction or mechanical reasons it stays initially in a given state as shown in Fig.1; then the plates are pressed under the external loading. We assume that the Coulomb's law of friction is valid in contact with coefficients of friction μ_1 and μ_2 at the upper and lower interfaces, respectively.
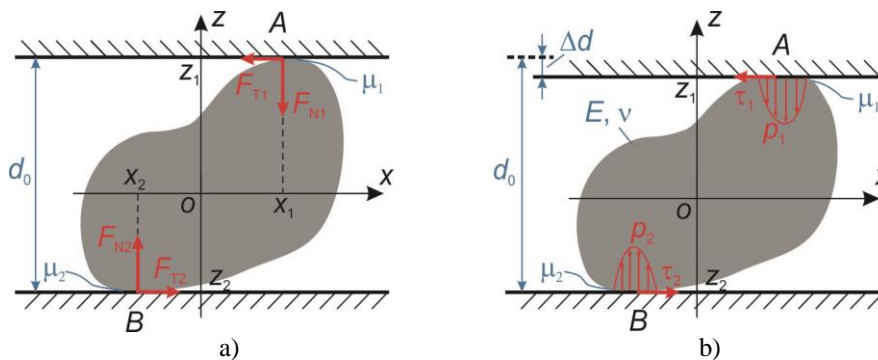
Fig. 1 A single particle trapped between two plates. (a) particle is rigid and concentrated normal and tangential forces F_N, F_T act on contact points A and B; (b) particle is deformable and loads are distributed stresses p and τ on areas

Under the loading, the particle may roll, rotate, or keep its initial state. If the particle is rigid, then the state depends only on the coefficient of friction and the geometry of the particle, not on the loading process.

2.1. Rigid particle

Let us consider a two-dimensional case as shown in Fig. 1a, or three-dimensional but the geometry of the particle is symmetric with respect to the xz-plane, so that only the moment around y-axis (perpendicular to xz-plane) has to be considered. The origin of the coordinates is located at the centroid of the particle. The normal and tangential forces acting on the particle at upper contact point A are defined as F_{N1} and F_{T1}, and forces at lower point B are F_{N2} and F_{T2}. Simply according to the equilibrium condition for the particle, we have

$$F_{N1} = -F_{N2}, F_{T1} = -F_{T2},$$ (1)

and total moment of these forces around the origin should be zero if the particle is unmoved

$$\sum M = F_{N1}x_1 + F_{N2}x_2 + F_{T1}z_1 + F_{T2}z_2 = 0,$$ (2)

which gives

$$\left|\frac{F_{T1}}{F_{N1}}\right| = \left|\frac{F_{T2}}{F_{N2}}\right| = \left|\frac{x_1 - x_2}{z_1 - z_2}\right| = \xi.$$ (3)

Following the Coulomb's law of friction, the tangential force at the sliding state is equal to normal force multiplying the coefficient of friction which is the maximal reachable value of tangential force. Therefore, by comparing the local coefficient of friction with the ratio in Eq. (3), we can predict the state of particle as follows:

$$\begin{cases} \mu_1, \mu_2 > \xi, & \text{sticking} \\ \mu_1 > \xi \text{ and } \mu_2 < \xi, & \text{rolling - } A \text{ sticking, } B \text{ sliding} \\ \mu_1 < \xi \text{ and } \mu_2 > \xi, & \text{rolling - } B \text{ sticking, } A \text{ sliding} \\ \mu_1, \mu_2 < \xi, & \text{rotation around origin } O \end{cases}$$ (4)

In this paper we define "rotation" as the rotation of the particle around its centroid, and "rolling" as the rotation around the contact point either in the upper or lower interface. If the coefficients of friction are same $\mu_1=\mu_2$, the particle will either rotate or keep unmoved:

$$\begin{cases} \mu > \xi, & \text{sticking} \\ \mu < \xi, & \text{rotation} \end{cases}.$$ (5)

From Eqs. (3) and (4), it follows that the state of particle under the loading depends only on the coefficient of friction and the geometry and orientation of particle. The similar behavior was discussed about kinematics of particles in [18].

2.2. Soft particle

If the body is deformable, the contact will be different. Firstly, the loads are not concentrated forces acting on some points, but distributed stresses on some areas. And the moment arms of the stresses are then related to the location of contact area. Furthermore,

due to the deformation of particle, there could be multi-contact spots in one contact interface during loading. As sketched in Fig. 1b, the equilibrium condition for the deformed particle in this case becomes

$$\Sigma F_z = \int p_{up}(x, y)\mathrm{d}A_{up} + \int p_{low}(x, y)\mathrm{d}A_{low} = 0$$

$$\Sigma F_x = \int \tau_{up}(x, y)\mathrm{d}A_{up} + \int \tau_{low}(x, y)\mathrm{d}A_{low} = 0$$

$$\Sigma M = \int p_{up}(x, y)x\mathrm{d}A_{up} + \int p_{low}(x, y)x\mathrm{d}A_{low}$$

$$+ \int \tau_{up}(x, y)z\mathrm{d}A_{up} + \int \tau_{low}(x, y)z\mathrm{d}A_{low} = 0$$

(6)

The third equation in (6) is the equilibrium condition for the moment of the normal and tangential stresses around the centroid of particle. It is noted that the centroid may change a bit due to the deformation during the loading.

The stresses in contact have to be numerically calculated using the BEM. For a clear description of numerical simulation, we mention two available basic functions in the BEM: (1) normal pressure distribution p can be calculated with given indentation depth d and the geometry of indenter (particle in this study); (2) tangential stress τ can be calculated with the given tangential displacement.

The latter one has been already applied to the partial sliding with the Coulomb's law of friction: under the normal load a deformable body is pressed on a rigid plane and then the plane moves a bit in tangential direction; then the tangential displacement of the body at the contact area can be calculated as well as the tangential stress. As shown in Fig. 2 with an example of a tilted ellipsoid, there will be a stick region in the middle of contact area and a relative slip region at the boundary of contact (Fig. 2b). The criterion can be formulated as follows: when the tangential stress is smaller than normal stress multiplying the coefficient of friction $\tau < \mu p$, the incremental tangential displacement of the surface in contact area Δu_x is equal to that of indenter Δu_{x0}. These elements are in the stick region. Otherwise, the elements are in a state of slip:

$$\Delta u_x = \Delta u_{x0}, \quad \text{in stick region}$$
$$\tau = \mu p, \qquad \text{in slip region}$$

(7)

a)   b)   c)
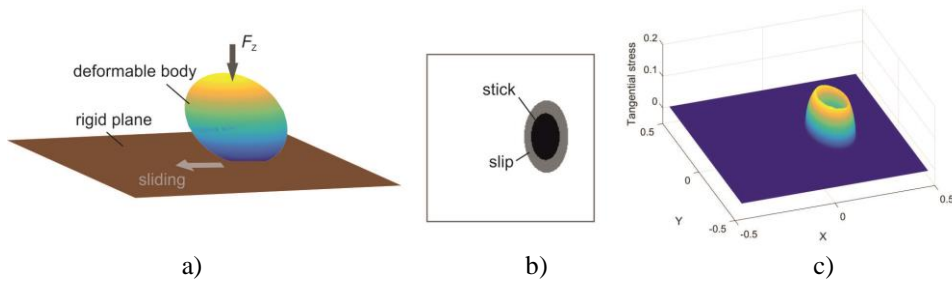
Fig. 2 Simulation example of partial sliding of a deformable ellipsoid on a rigid plane (a) Illustration of contact: the plane has a contact with ellipsoid under the normal load and then moves a little in tangential direction. There is a stick (black) and a slip (gray) region in contact area (b). The tangential stress distribution is shown in (c)

We consider a soft particle squeezed by two plates. The external normal loading on plates is given and the two parallel plates are fixed in horizontal direction so they can move only in vertical direction. With the existing functions described above we can further realize the following calculations iteratively: (1) the deformation of particle and normal stresses can be obtained with the given normal force; (2) the tangential stress and a stick and slip region can be calculated with the given tangential force under the Coulomb's law of friction (as shown in Fig. 2). In more detail, the simulation of particle contact is the following. Under known external load F_z the normal stresses and contact areas on upper and lower interfaces p_{up}, p_{low}, A_{up}, A_{low} and deformation of particle can be easily calculated, also the moment of normal pressures

$$M_{p} = \int p_{up}(x, y)x \mathrm{d}A_{up} + \int p_{low}(x, y)x \mathrm{d}A_{low} \ . \tag{8}$$

If the coefficients of friction in the upper and lower interfaces are the same, $\mu_{up} = \mu_{low} = \mu$, one can simply check whether the particle would rotate. The moment of normal load urges the particle to rotate, but the frictional force in tangential direction will hinder this movement. Because the plates are rigid, the moment arms of tangential stress are the same in each contact interface. The state of particle can be determined by comparing the tangential force needed for rotation F'_x which is equal to

$$F_{x}^{'} = \frac{M_{p}}{(z_{1} - z_{2})}, \tag{9}$$

and maximal achievable tangential force μF_z (sliding frictional force):

$$\text{Particle will rotate, if } F_{x}' > \mu F_{z}, \tag{10}$$

where z_1-z_2 is the moment arm of tangential forces. If the condition (10) is not met, the particle will generally keep unmoved but a partial sliding exists. Then the tangential stress distribution and a stick and slip region can be calculated with tangential force F'_x in Eq. (9).

For different coefficients of friction, the criterion is basically same. The tangential force needed for rotation F'_x is still obtained from the results of normal contact in Eq. (9); then by comparing it with the value of μF_z for the upper and lower interfaces, respectively, the state of particle is determined:

$$\begin{aligned} &F_{x}' > \mu_{up} F_{z} \text{ and } F_{x}' > \mu_{low} F_{z}, \quad \text{rotation} \\ &F_{x}' > \mu_{up} F_{z} \text{ and } F_{x}' < \mu_{low} F_{z}, \quad \text{rolling around upper contact spot} \\ &F_{x}' < \mu_{up} F_{z} \text{ and } F_{x}' > \mu_{low} F_{z}, \quad \text{rolling around lower contact spot} \\ &F_{x}' < \mu_{up} F_{z} \text{ and } F_{x}' < \mu_{low} F_{z}, \quad \text{sticking} \end{aligned} \tag{11}$$

It is noted that the contact spot is an area in this case, so if the body size is much larger than the size of contact, one can simply let the particle roll around the center of the sticking area.

3. EXAMPLES OF NUMERICAL SIMULATION

In this section, we illustrate the above method with a few examples.

3.1. Cases with the same coefficients of friction

Firstly, a simple case with the same coefficients of friction is simulated, $\mu_{up} = \mu_{low} = \mu$. The particle has only two states: rotation or keeping unmoved. In the simulation external normal load F_N is set to increase linearly. The particle has a "potato" shape and its geometry is symmetric with respect to the shown plane. It is numerically generated by superposition of ellipsoid and sine waves with comparable wavelength and amplitude. In each compression step, the contact area, a stick and slip region and the tangential force are calculated. Fig. 3a shows the dependence of the ratio of tangential force and normal force multiplied by coefficient of friction $F_T/(\mu F_N)$ on the compression distance. The distance of the horizontal coordinate is normalized by initial gap d_0. The value of $F_T/(\mu F_N)$ indicates the state of particle: $F_T/(\mu F_N)<1$ (gray region) for a general sticking state (actually in a partial sticking state), and $F_T/(\mu F_N)=1$ (red line) for rotation.

It is seen that the particle is in a state of stick at the first contact under a very tiny load. If the particle is rigid, it will always stay in this state no matter how large the load is. But in this case of a soft body, we can see that the particle has a few rotations during the compression. Observing states *a* and *b* marked in the curve (or similar series *c-d-e*) and corresponding contact areas in Fig.3b, the particle has the following behavior: initially it is in a state of sticking, then the tangential force increases during compression and approaching to the value of μF_N while the sticking region in the contact area shrinks until rotation occurs. This phenomenon repeats several times and finally the particle stays "stable" between the plates while the tangential force decreases (state *f*).
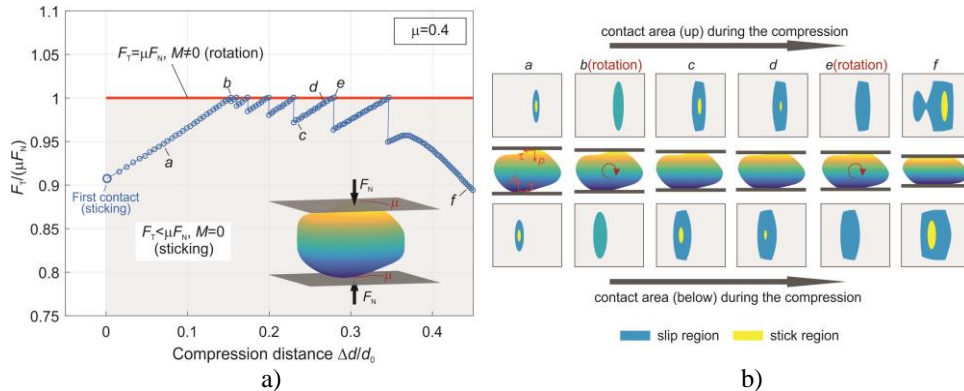
Fig. 3 Simulation of a single particle in compression: (a) dependence of $F_T/(\mu F_N)$ on the compression distance; (b) contact configurations corresponding to the states marked in Fig.3a

Examples with smaller values of coefficient of friction are shown in Fig. 4. Other parameters remain unchanged. It is observed that the particle rotates at the first contact: after the rotation by an angle 6° in the case of $\mu=0.3$ and angle 9° in the case of $\mu=0.2$ it comes into the state of sticking. For $\mu=0.2$ the sticking state keeps in the whole compression process after the

initial rotation. It is noted that the tangential force in this case becomes negative at the larger load, which indicates that the tangential force decreases during compression and will act on the surface in the opposite direction.
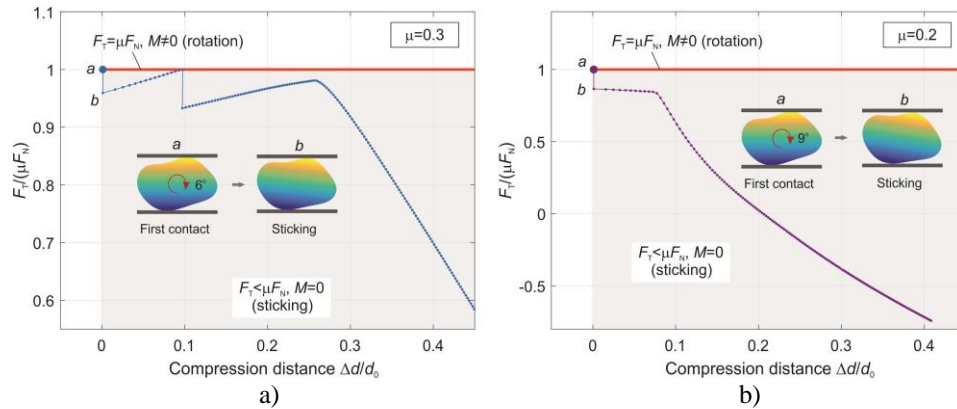
Fig. 4 Examples with smaller coefficient of friction: (a) μ=0.3; (b) μ=0.2

3.2. Cases with different coefficients of friction

Now we consider a case with different coefficients of friction, μ_{up}=0.2 and μ_{low}=0.4. The external normal loading is the following: the normal force keeps constant till the particle reaches a stable state and then increases linearly. From Fig. 5a it is seen that under the load the upper interface is in a slip state where the value of $F_T/(\mu_{up}F_N)$ is one (blue curve with stars) and lower interface in a sticking state where $F_T/(\mu_{low}F_N)$ is smaller than one and decreases (red curve with triangles). This rolling continues to a stable state - point "*b*" where the particle sticks in both interfaces (Fig. 5b). With an increasing normal loading the particle is further compressed without rotation (state *c*).
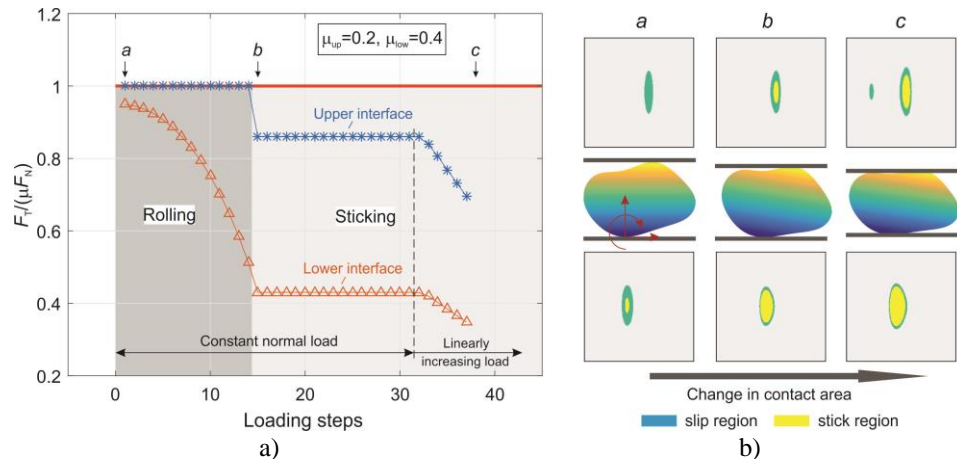
Fig. 5 Simulation examples with different coefficient of friction in the upper and lower interfaces. (a) State of particle during the loading; (b) three contact configurations corresponding to the states marked in Fig. 5(a)

4. CONCLUSION

We studied a simple case of third body particle: a single deformable particle is compressed by two parallel plates. The frictional contact of the particle was numerically simulated by the FFT-assisted BEM. Unlike the rigid particle, the soft particle during the compression may change its state, for example from sticking to rolling. The normal and tangential stress distributions, deformation of the particle, and stick and slip regions were calculated. By comparing the tangential force needed for slipping and the maximal achievable tangential force, the state of particle state was determined. Applications of this method were shown with a few examples with the same and different coefficients of friction in the upper and lower interfaces. This method can be further developed for the simulation of kinematics of multiple third-body particles including various sizes of particles.

REFERENCES

1. Greenwood, J.A., 2020, *Metal transfer and wear*, Frontiers in Mechanical Engineering, 6, 62.
2. Stempflé, P., Von Stebut, J., 2006, *Nano-mechanical behaviour of the 3rd body generated in dry friction - Feedback effect of the 3rd body and influence of the surrounding environment on the tribology of graphite*, Wear, 260, pp. 601–614 .
3. Pellegrin, D.V.De, Torrance, A.A., Haran, E., 2009, *Wear mechanisms and scale effects in two-body abrasion*, Wear, 266, pp. 13–20.
4. Ostermeyer, G.P., 2003, *On the dynamics of the friction coefficient*, Wear, 254, 852–858.
5. Müser, M.H., Wenning, L., Robbins, M.O., 2001, *Simple microscopic theory of Amonton's laws for static friction*, Physical Review Letters, 86, pp. 1295–1298.
6. Shi, J., Chen, J., Wie, X., Fang, L., Sun, K., Sun, J., Han, J., 2017, *Influence of normal load on the three-body abrasion behaviour of monocrystalline silicon with ellipsoidal particle*, Royal Society of Chemistry Advances, 7, pp. 30929–30940.
7. Fang, L., Liu, W., Du, D., Zhang, X., Xue, Q., 2004, *Predicting three-body abrasive wear using Monte Carlo methods*, Wear, 256, pp. 685–694.
8. Tergeist, M., Müller, M., Ostermeyer, G.P., 2013, *Modeling of the wear particle flow in tribological contacts*, Proceeding in Applied Mathematics and Mechanics, 13, pp. 123–124.
9. Deng, F., Tsekenis, G., Rubinstein, S.M., 2019, *Simple law for third-body friction*, Physical Review Letters, 122, 135503.
10. Popov, V.L., 2020, *Coefficients of restitution in normal adhesive impact between smooth and rough elastic bodies*, Reports in Mechanical Engineering, 1(1), pp. 103-109.
11. Wang, Q., Sun, L., Zhang, X., Liu, S., Zhu D., 2020, *FFT-Based Methods for Computational Contact Mechanics*, Frontiers in Mechanical Engineering, 6, 61.
12. Putignano, C., Afferrante, L., Carbone, G., Demelio, G., 2012, *A new efficient numerical method for contact mechanics of rough surfaces*, International Journal of Solids and Structures, 49, pp. 338–343.
13. Rey, V., Anciaux, G., Molinari, J.F., 2017, *Normal adhesive contact on rough surfaces: efficient algorithm for FFT-based BEM resolution*, Computational Mechanics, 60, pp. 69–81.
14. Liu, S., Wang, Q., Liu, G., 2000, *A versatile method of discrete convolution and FFT (DC-FFT) for contact analyses*, Wear, 243, pp. 101–111.
15. Li, Q., Pohrt, R., Lyashenko, I.A., Popov, V.L., 2019, *Boundary element method for nonadhesive and adhesive contacts of a coated elastic half-space*, Proc. Inst. Mech. Eng. Part J J. Eng. Tribol., 234, pp. 73–83.
16. Li, Q., Popov, V.L., 2017, *Boundary element method for normal non-adhesive and adhesive contacts of power-law graded elastic materials*, Computational Mechanics, 61, pp. 319–329.
17. Benad, J., 2020, *Calculation of the BEM integrals on a variable grid with the FFT*, Frontiers in Mechanical Engineering, 6, 32.
18. Bilz, R., de Payrebrune, K.M., 2019, *Analytical investigation of the motion of lapping particles*, Proceeding in Applied Mathematics and Mechanics, 19, e201900076.